The theoretical results (dashed line in Fig. 3D) are calculated for the electron temperature in the experiment (70 mK), as determined from the temperature dependence of Coulomb blockade oscillations (*11*). Although no adjustable parameters are used in the theory, the agreement between the experimental and theoretical results is excellent. The output high (V_{OH}) and output low (V_{OL}) show a clear separation, as required for digital logic. The first and last four input steps are grouped separately, with A as the programming input, to illustrate AND and OR operations. The AND operation is carried out for $A = 0$, for which we see that the output is high only when the remaining two inputs are also high. The OR operation is performed when $A = 1$, for which the output is high when either of the other two inputs is high. These data confirm majority gate operation and thus demonstrate a logic gate that requires only two electrons to function.

The gap between V_{OH} and V_{OL} would be larger for either lower temperatures or smaller capacitances. Thermal smearing of the charge states of the dots results in a less than complete polarization of the cell. Therefore, the performance of the gate could be improved by lowering the temperature. However, a better way is to reduce the dot capacitance (by reducing the size of the dots), which will raise the energy of the excited states. When all capacitances are reduced by a factor of 10, the calculated output characteristic shows increased separation between V_{OH} and V_{OL} and negligible output deviations for all input combinations. QCA logic gates using a molecular implementation will not only yield greater performance, but will also operate at room temperature (*12*).

Some key issues must be addressed to determine the response of the majority gate when it is integrated in a real QCA circuit. In QCA arrays, each cell responds to the polarizations of neighboring cells. Therefore, we must justify that the voltages applied to the central cell gates in our majority gate experiment produce the same effects as electrons switching in neighboring cells.

We performed two experiments to demonstrate that our input voltages have the same effect as that of actual electron switching in input cells A, B, and C. First, we found the potential swing due to an electron switching from one dot to another. We applied a differential voltage between gates 3 and 4 ($V_3 = -V_4$) to induce electron switching in D_3D_4 (inset, Fig. 4A). As an electron moves from D_4 to D_3, the potential of the bottom dot undergoes a positive shift due to removal of an electron, while the potential of the top dot undergoes a negative shift due to addition of an electron. The differential potential swing ($\Phi_{D4} - \Phi_{D3}$) for this switching is positive (Fig. 4A), with theory closely matching the measured data [the calculated differential potential swing ($\Phi_{D2} - \Phi_{D1}$) is the same when the bias is applied between gates 1 and 2]. The input signals applied to the gates in the majority gate demonstration (Fig. 3) have the same amplitudes as that shown in Fig. 4A, scaled by C_J/C_G to compensate for differences in capacitance.

Next, to demonstrate that the application of "simulated" dot potentials to the gates of the cell mimics an electron switching in a neighboring cell, we applied the differential potential extracted in the previous experiment directly to gates 3 and 4 (with the weighting factor C_J/C_G) and measured the differential potentials between D_3 and D_4. This result is compared to that due to an actual electron switching in nearby dots D_1D_2. Figure 4B shows the change in differential potential of D_3D_4 caused by the two mechanisms as a function of time (insets, Fig. 4B), with the data confirming that the response of D_3D_4 is similar when switched by either the simulated potential or a real electron. This is as expected because charge modulations induced on D_3D_4 by the two mechanisms are the same; that is, $V_3C_G = \Phi_{D1}C_J$ and $V_4C_G = \Phi_{D2}C_J$. These results confirm that using the simulated dot potentials for the inputs in our majority gate experiment is indeed a reliable indicator of how a majority gate would respond when integrated in a QCA circuit.

References and Notes

1. C. S. Lent and P. D. Tougaw, *Proc. IEEE* **85**, 541 (1997).
2. ———, W. Porod, *Appl. Phys. Lett.* **62**, 714 (1993).
3. C. S. Lent and P. D. Tougaw, *J. Appl. Phys.* **75**, 4077 (1994).
4. A. O. Orlov, I. Amlani, G. H. Bernstein, C. S. Lent, G. L. Snider, *Science* **277**, 928 (1997); I. Amlani, A. O. Orlov, G. L. Snider, C. S. Lent, G. H. Bernstein, *Appl. Phys. Lett.* **72**, 2179 (1998).
5. In an integrated QCA circuit, a clocking scheme is used to control the direction of information flow. See (*1*).
6. K. K. Likharev, *IBM J. Res. Dev.* **42**, 144 (1988).
7. P. Lafarge *et al.*, *Z. Phys. B* **85**, 327 (1991); I. Amlani, A. O. Orlov, C. S. Lent, G. L. Snider, G. H. Bernstein, *Appl. Phys. Lett.* **71**, 1730 (1997).
8. G. L. Snider *et al.*, unpublished data; G. H. Bernstein, I. Amlani, A. O. Orlov, C. S. Lent, G. L. Snider, unpublished data.
9. T. A. Fulton and G. H. Dolan, *Phys. Rev. Lett.* **58**, 109 (1987).
10. G. L. Snider *et al.*, *Solid State Electron.* **42**, 1355 (1998).
11. H. Grabert and M. H. Devoret, Eds., *Single Electron Tunneling* (Plenum, New York, 1992), p. 181.
12. C. S. Lent, P. D. Tougaw, W. Porod, *Proceedings of Workshop on Physics and Computation* (IEEE Computer Press, Los Alamitos, CA, 1994), vol. 5.

13. Supported in part by the Defense Advanced Research Projects Agency, the Office of Naval Research (grant N0014-95-1-1166), and NSF. We thank W. Porod and J. Merz for helpful discussions.

24 November 1998; accepted 19 February 1999

Remote Triggering of Waves in an Electrochemical System

J. Christoph, P. Strasser,* M. Eiswirth, G. Ertl

In the potentiostatic electrochemical oxidation of formic acid on a platinum ring electrode under bistable conditions, an appropriate perturbation at one location of the ring can cause the emergence of a wave on the opposite side (remote triggering). These findings can be rationalized in terms of the nonlocal coupling function of the system and are theoretically reproduced by solution of the corresponding reaction-migration equation.

Trigger waves are a widespread phenomenon, both in conservative systems (such as ripples on the surface of water) and in dissipative systems [such as active chemical media (*1*), nerve axons, or heart tissue (*2*, *3*)]. They typically originate from the location where a perturbation (trigger) has been applied, be it a stone thrown into a pond or an electrical stimulus applied to an axon. If, however, coupling between different parts is nonlocal, that is, when any change of state affects instantaneously the whole system (*4*, *5*), the necessity for local causality will no longer exist. We present here the results and theoretical interpretation of an electrochemical experiment in which a local perturbation causes the initiation of a trigger wave in a remote region.

The experiment was performed with the electrochemical oxidation of formic acid on platinum (*6*), which exhibits for a certain range of parameters bistability between a passive (OH-poisoned) and an active (high-current)

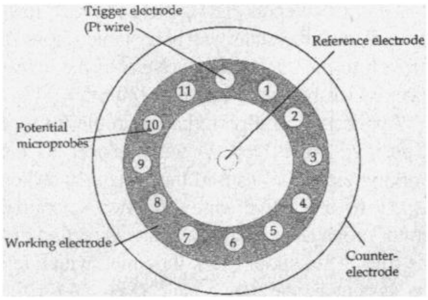

Fig. 1. Schematic view of the electrode setup. The potential microprobes (1 through 11) are separated by 30° angles, and the perturbations were applied with a Pt wire.

Fritz-Haber-Institut der Max-Planck-Gesellschaft, Faradayweg 4-6, D-14195 Berlin, Germany.

*To whom correspondence should be addressed. E-mail: strasser@fhi-berlin.mpg.de

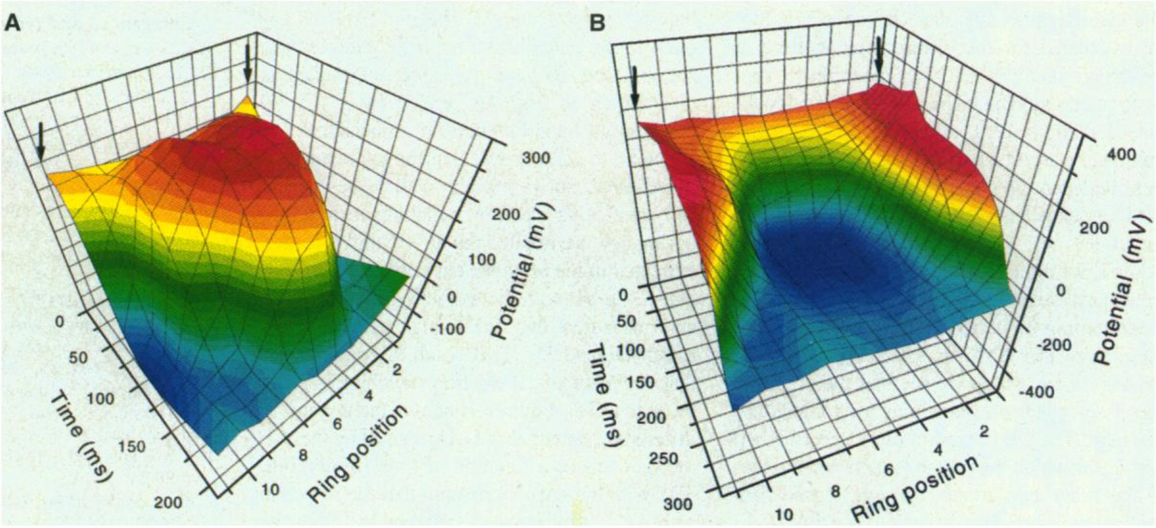

Fig. 2. Space-time plots of the potential distribution on the Pt ring electrode during passive-active transitions. The ring position refers to the probes 1 through 11 as in Fig. 1 (the electrolyte was 0.1 M HCOONa/0.05 M H_2SO_4). (**A**) Local triggering: A pulse of +3 V and 0.1-s duration was applied to the perturbing electrode (position 12, not shown), triggering two propagating fronts at positions 1 and 11 (E = 320 mV). (**B**) Remote triggering: pulse of –5 V and 0.1-s duration (E = 300 mV). Activation starts at position 6 opposite to the perturbation.

state. A bistable system represents the simplest dissipative medium in which trigger waves can be created. Typically, a sufficiently strong localized perturbation causes a local transition from the metastable (for example, the passive) state to the other (the active) one, which then spreads through front propagation until the whole system has been switched to the other state. A perturbation with opposite sign (which would make the state even more passive) would not be expected to have any effect. This latter conclusion is not necessarily valid, as is demonstrated by the results given below.

The experimental setup is outlined in Fig. 1. A Pt ring of 32-mm inner diameter and 42-mm outer diameter was used as a working electrode, and a Hg/Hg_2SO_4 reference electrode was placed into the center of the ring. A Pt wire served as a counterelectrode situated 60 mm above the plane of the other two electrodes. To monitor the propagation of fronts, we placed 11 potential microprobes (consisting of Hg/Hg_2SO_4 reference electrodes in glass capillaries) about 0.5 mm above the working electrode; they measured the potential drop across the electric double layer. At the 12th position, a Pt wire (0.1 mm thick) was used to apply perturbations. The working electrode was prepared in the passive state by scanning the voltage to a high value E = 750 mV versus Hg/Hg_2SO_4 and then lowering E until the state was metastable (close to but before the spontaneous return to the active state, which occurred at about 220 mV).

Application of a perturbation in the form of a positive pulse (+3 V with respect to the working electrode) caused the system to switch locally to the active state, and two activation fronts propagated along opposite directions of the ring. After about 0.2 s, they met, which left the system in the active state (Fig. 2A). (The passive state corresponds to a high potential drop across the electric double layer; thus, a positive pulse outside the double layer tends to destroy it.) Up to this point, the system behaved qualitatively just as expected for local coupling. However, the effect of a negative pulse applied to the same position, which should have locally stabilized the double layer, is shown in Fig. 2B. Indeed, the potential drop temporarily increased slightly at positions 1 and 11, but on the opposite side of the perturbation (that is, starting at position 6), activation occurred, followed by front propagation. In both cases shown, the front velocity was nonuniform, first spreading very rapidly and then decelerating before reaccelerating just before the fronts met.

The dominant coupling process in electrochemical systems is ion migration under the influence of the electric field (electromigration) rather than diffusion (*5*, *7*). Every electrochemical reaction produces charges that balance very quickly because no net charges can be built up in the electrolyte. The electroneutrality condition requires that for every surface element of the double layer, the capacitive and faradaic (reaction) currents (i_{cap} and i_{reac}, respectively) are balanced by the migration current (i_{mig}) (Kirchhoff's law):

$$i_{cap} = -i_{reac} + i_{mig} \qquad (1)$$

Evaluation of the terms in Eq. 1 results in a general reaction-migration equation (*7–10*) for the double-layer potential $u(x, t)$, where x is the spatial coordinate along the electrode and t is time. For the present case (ring electrode and potentiostatic control), it takes the form

$$C\partial_t u = -i_{reac}(u) + \frac{E-u}{R} + \kappa \int_0^{2\pi} H(|x-x'|)[u(x') - u(x)]dx' \qquad (2)$$

where C is the double-layer capacity, R is the resistance of the solution, E is the external voltage, κ is the conductivity of the electrolyte, and H is the coupling function.

Thus, the migration current is composed of a local term $(E - u)/R$ and a coupling term that in general couples every point of the electrode to every other one. The coupling function $H(|x - x'|)$ denotes how strongly two points at distance $|x - x'|$ are coupled to each other. It can be derived from electrodynamic principles (*8*, *10*) and depends only on the geometry of the electrode setup (in particular, it is very sensitive to the distance between the working and the reference electrodes). Its form for a pointlike reference electrode at the center of a ring with the counterelectrode at infinity has been computed numerically (Fig. 3). It falls off rapidly and becomes negative with increasing distance $|x - x'|$.

Numerical simulations were carried out with Eq. 2 with the coupling function H of Fig. 3 and a simple bistable form for the local part; that is, i_{reac} is a third-order polynomial in u (*11*). The resulting passive-active transitions are shown in Fig. 4, A and B. An initial perturbation of u to a lower value resulted in a local transition (Fig.

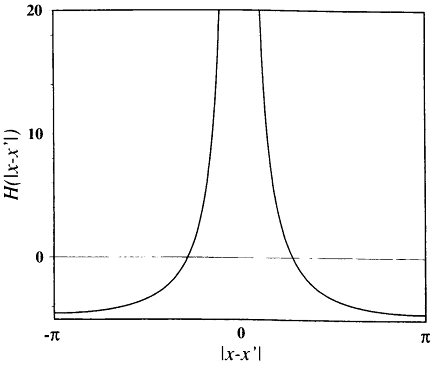

Fig. 3. Computed coupling function $H(|x - x'|)$ for a ring electrode with an inner diameter of 0.8 and an outer diameter of 1.0 and a pointlike reference electrode at the ring center (counterelectrode assumed at infinity). At a large distance, the coupling becomes negative, which means that activation at point x favors passivation at x' and vice versa.

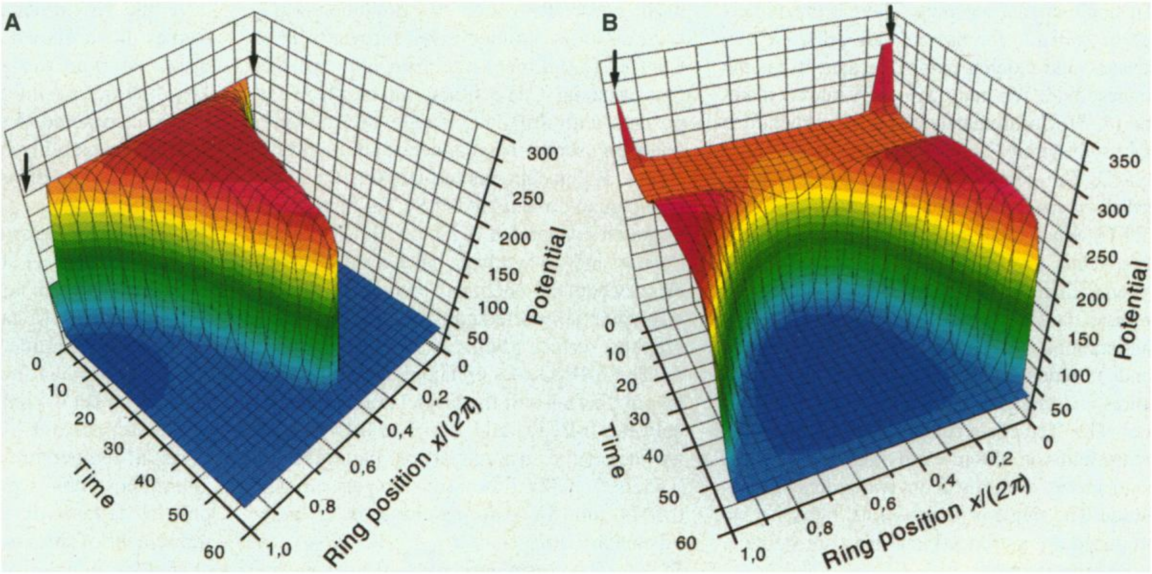

Fig. 4. Simulated passive-active transitions with the reaction-migration Eq. 2 in the bistable regime: periodic boundary conditions (corresponding to a ring), with perturbation applied in the region. 0 = 2π ($i_{\mathrm{real}} = \Sigma_{i=1}^{3} a_i u^i$, $a_1 = 5.5932$, $a_2 = -0.04725$, $a_3 = 10^{-4}$; $E = 233.5$, $R = 1.5$, $\kappa = 0.057$, $C = 1$.) All quantities are given in dimensionless units. The passive state corresponds to a potential u of 230, and the active state corresponds to a potential u of 30. (**A**) Local triggering, with u locally lowered by 126 over an angle of 30° in the initial conditions. (**B**) Remote triggering, with u locally increased by 250 over a 45° angle in the initial conditions (plot starts t = 0.2 s).

4A), whereas the opposite perturbation triggered the transition 180° away (Fig. 4B), in complete agreement with the experiment.

The remote triggering of electrochemical reaction fronts provides a direct experimental demonstration of the nonlocal nature of migration coupling (*5*). It can be easily rationalized in terms of the coupling function H (Fig. 3), which is positive for small distances (thus enabling front propagation) but negative further away, allowing a local perturbation with the "wrong" sign to manifest itself at a remote distance, where its sign is reversed by the coupling. Nonlocal phenomena are obviously not restricted to bistability but are expected to manifest themselves also for more complex local dynamics [compare with (*12*, *13*)].

The apparently "instantaneous" coupling observed arises from the slow time scale of the reaction (about 0.1 s for the removal of the passivating OH layer), whereas the electric field effects spread with the velocity of light (less than 10^{-9} s across the system). Hence, nonlocal effects, such as remote triggering, are expected whenever a very fast coupling occurs in a system with slow local dynamics. This includes not only electrochemical reactions but also biochemical processes coupled by electric field effects.

References and Notes

1. R. Kapral and K. Showalter, Eds., *Chemical Waves and Patterns* (Kluwer Academic, Dordrecht, Netherlands, 1995).
2. Special issue on Wave Patterns in Chemical and Biological Systems, H. L. Swinney and V. I. Krinsky, Eds., *Physica D* **49** (no. 1/2) (1991).
3. A. T. Winfree, *When Time Breaks Down* (Princeton Univ. Press, Princeton, NJ, 1987).
4. J. D. Murray, *Mathematical Biology* (Springer-Verlag, Berlin, 1990).
5. K. Krischer, in *Modern Aspects of Electrochemistry*, vol. 32, B. E. Conway, J. O. Bockris, R. White, Eds. (Plenum, New York, in press).
6. P. Strasser, M. Lübke, F. Raspel, M. Eiswirth, G. Ertl, *J. Chem. Phys.* **107**, 979 (1997).
7. G. Flätgen and K. Krischer, *Phys. Rev. E* **51**, 3997 (1995); *J. Chem. Phys.* **103**, 5428 (1995).
8. J. Christoph, thesis, Freie Universität Berlin (1999).
9. P. Grauel, J. Christoph, G. Flätgen, K. Krischer, *J. Phys. Chem. B* **102**, 10264 (1998).
10. J. Christoph, R. Otterstedt, M. Eiswirth, N. I. Jaeger, J. L. Hudson, *J. Chem. Phys.*, in press.
11. N. Mazouz, G. Flätgen, K. Krischer, *Phys. Rev. E* **55**, 2260 (1997).
12. J. C. Sayer and J. L. Hudson, *Ind. Eng. Chem. Res.* **34**, 3246 (1995).
13. Z. Fei, R. G. Kelly, J. L. Hudson, *J. Phys. Chem.* **100**, 18986 (1996).

29 December 1998; accepted 3 March 1999

Electrodeposited Ceramic Single Crystals

Jay A. Switzer,* Mark G. Shumsky, Eric W. Bohannan

Single-crystal films are essential for devices because the intrinsic properties of the material, rather than its grain boundaries, can be exploited. Cubic bismuth oxide has the highest known oxide ion mobility, which makes it useful for fuel cells and sensors, but it is normally only stable from 729° to 825°C. The material has not been previously observed at room temperature. Single-crystal films of the high-temperature cubic polymorph of bismuth oxide were epitaxially electrodeposited from an aqueous solution onto single-crystal gold substrates. The 35.4 percent lattice mismatch was accommodated by forming coincidence lattices in which the bismuth oxide film was rotated in relation to the gold substrate. These results provide a method for producing other nonequilibrium phases that cannot be accessed by traditional thermal processing.

Electrodeposition can be used to produce nonequilibrium materials and architectures that cannot be accessed by traditional thermal processing. Nonequilibrium crystal structures can be stabilized by producing nanometer-scale crystallites or by epitaxially depositing the material onto a template with a crystal structure similar to the one desired. We have previously used electrodeposition to produce nonequilibrium layered nanostructures and superlattices of metal oxides that showed quantum confinement effects (*1*–*6*). Here, we show that single-crystal films of the high-temperature cubic polymorph of bismuth oxide (δ-Bi_2O_3) can be epitaxially electrodeposited onto cubic single-crystal Au substrates. The system achieves epitaxy by forming coincidence lattices in which the δ-Bi_2O_3 overlayer is rotated in relation to the

---

University of Missouri–Rolla, Department of Chemistry and Graduate Center for Materials Research, Rolla, MO 65409–1170, USA.

*To whom correspondence should be addressed. E-mail: jswitzer@umr.edu